Transport and optical properties of tin δ-doped GaAs structures

V. A. Kul'bachinskiĭ, V. G. Kytin, R. A. Lunin, V. G. Mokerov, A. P. Senichkin, A. S. Bugaev, A. L. Karuzskiĭ, and A. V. Perestoronin

M. V. Lomonosov Moscow State University, 119899 Moscow, Russia

R. T. F. van Schaijk and A. de Visser

Van der Waals Laboratory, University of Amsterdam, the Netherlands
(Submitted November 10, 1998; accepted for publication December 1, 1998)
Fiz. Tekh. Poluprovodn. **33**, 839–846 (July 1999)

The transport and optical properties of tin δ layers in GaAs are investigated as functions of the Sn concentration. The Shubnikov–de Haas and Hall effects are measured in the temperature range 0.4−12 K in magnetic fields up to 38 T. The band diagrams and quantum mobilities of electrons in the quantum-well subbands are calculated. Features associated with electronic transitions from quantum-well levels are found in the photoluminescence spectra of the structures. Oscillations of the resistance are observed in a magnetic field parallel to the δ layer and are attributed to features in the density of states at the Fermi level. © *1999 American Institute of Physics.* [S1063-7826(99)01607-5]

1. INTRODUCTION

One of the effective methods for obtaining a high concentration of two-dimensional electrons in semiconductor structures is δ doping, under which an impurity is concentrated in a very thin layer, which ideally consists of only one sheet of atoms. Silicon is usually used for δ doping. Tin has hitherto been used only to a small extent to δ dope GaAs because of its high capacity for surface segregation,[1] although, as a donor impurity, it is less amphoteric than silicon, which has been used traditionally to create *n*-type δ layers. The use of Sn makes it possible to obtain a high concentration of two-dimensional electrons in the δ layer. In the present work the transport and optical properties of tin δ layers on a singular surface are investigated in GaAs/GaAs(δ-Sn) structures as a function of the tin concentration. Scrutiny of the results of the tin δ doping of singular surfaces is important for comparison with data on the tin δ doping of vicinal (or high-index) gallium arsenide surfaces, which are promising for creating one-dimensional electron channels.[2,3]

2. SAMPLES AND MEASUREMENT METHOD

Tin δ-doped GaAs structures grown by molecular-beam epitaxy were investigated in this work. An *i*-GaAs buffer layer (240 nm) was grown on a semi-insulating (001) GaAs(Cr) substrate, and then a tin δ layer was deposited on the surface at $T_S \approx 450\,^{\circ}\mathrm{C}$ with an increased flow of As and capped by an *i*-GaAs layer with a thickness of 40 nm and a GaAs:Si contact layer (having a silicon concentration of $1.5\times10^{18}\,\mathrm{cm}^{-3}$) with a thickness of 20 nm. The tin doping level varied from $N_D = 2.97\times10^{12}\,\mathrm{cm}^{-2}$ in sample 1 to $N_D = 2.67\times10^{14}\,\mathrm{cm}^{-2}$ in sample 6. Some parameters of the samples are listed in Table I. The measurements were performed both on samples in the form of a double Hall bridge and on square samples.

The temperature dependence of the resistance was measured in the temperature range $0.4 < T < 300$ K. The Hall effect and the magnetoresistance were investigated at $0.4 < T < 12$ K in fixed magnetic fields up to 10 T and in pulsed fields up to 38 T. The pulsed magnetic-field facility of the University of Amsterdam was used for the measurements in magnetic fields up to 38 T. The measurements of the low-temperature photoluminescence spectra were performed at 4.2 K using an MDR-3 spectrometer and a photomultiplier operating in the photon-counting mode with optical excitation by the output of an argon laser (the wavelength was 514.5 nm, the radiated power was 7 mW, and the spot diameter was 1 mm).

3. CONDUCTANCE AND MAGNETORESISTANCE OF THE STRUCTURES INVESTIGATED

The resistance of sample 1 with a relatively small electron concentration increases as the temperature is lowered from room temperature to liquid-helium temperature (Fig. 1). The resistance of the heavily doped samples (4–6) decreases with decreasing temperature to a certain temperature (which decreases with increased doping of the sample) and then increases. As can be seen from Fig. 1, the resistance drops with increasing impurity concentration.

The Hall measurements showed that the Hall coefficient is constant in all of the samples in the range of magnetic fields investigated and does not depend on temperature in the range $0.4 < T < 12$ K. The values of the Hall electron concentration n_H obtained vary from $1.74\times10^{12}\,\mathrm{cm}^{-2}$ in sample 1 to $8.35\times10^{13}\,\mathrm{cm}^{-2}$ in sample 6 (see Table I), and the Hall mobility equals $1080-1940\ \mathrm{cm}^2/(\mathrm{V}\cdot\mathrm{s})$ in different samples at liquid-helium temperature.

Negative magnetoresistance was observed in all the samples at low temperatures in magnetic fields equal to $B < 0.2$ T. It was quadratic in weak magnetic fields and loga-

TABLE I. Tin concentration N_D, sum of the electron concentrations n_{SdH} in all the subbands determined from the Shubnikov–de Haas effect, and Hall concentration n_H for different samples at $T=4.2$ K.

Sample No.	N_D, 10^{12} cm^{-2}	Σn_{SdH}, 10^{12} cm^{-2}	n_H, 10^{12} cm^{-2}
1	2.97	2.75	1.74
2	8.91	8.73	3.59
3	26.7	7.30	2.63
4	29.7	7.80	10.4
5	89.1	8.09	8.35
6	267	45.3	83.5

rithmically dependent on magnetic induction in strong fields. The absolute value of the negative magnetoresistance decreases with increasing tin concentration in the δ layer. The Shubnikov–de Haas effect was observed in the structures investigated at low temperatures in strong magnetic fields. As an example, Fig. 2 shows the oscillations of the transverse magnetoresistance of samples 2 and 6, and Fig. 3 shows the Fourier transform of the oscillations of $\Delta R(H)$ in a reversed magnetic field for samples 2 and 4–6. Measurements of the dependence of the oscillation frequency on the tilt angle of the magnetic field showed that the oscillations are observed from two-dimensional carriers.

The two-dimensional electron concentrations in the quantum-well subbands determined from the maxima in the Fourier spectra are presented in Table II. It can be seen from Table I that the free-electron concentration Σn_{SdH} in samples 1 and 2 is approximately equal to the concentration of tin introduced N_D. As the concentration of tin introduced is increased, the free-electron concentration does not vary significantly (samples 3 to 5 in Table I). The positions of the maxima in the Fourier spectra in Fig. 3a are approximately identical for samples 2, 4, and 5, although the amplitudes of the peaks differ because of the different distributions of the electron mobilities among the subbands in these samples. The sum of the two-dimensional concentrations in four size-quantized subbands in samples 2–5 is equal to roughly

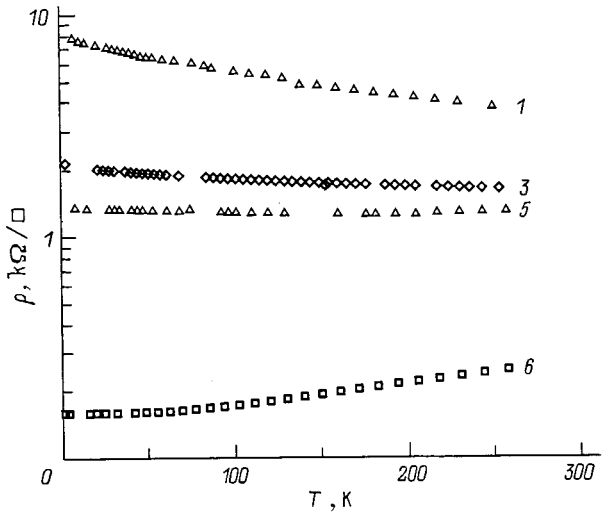

FIG. 1. Temperature dependence of the resistivity ρ (resistance per square) in samples 1, 3, 5, and 6 (see Table I).

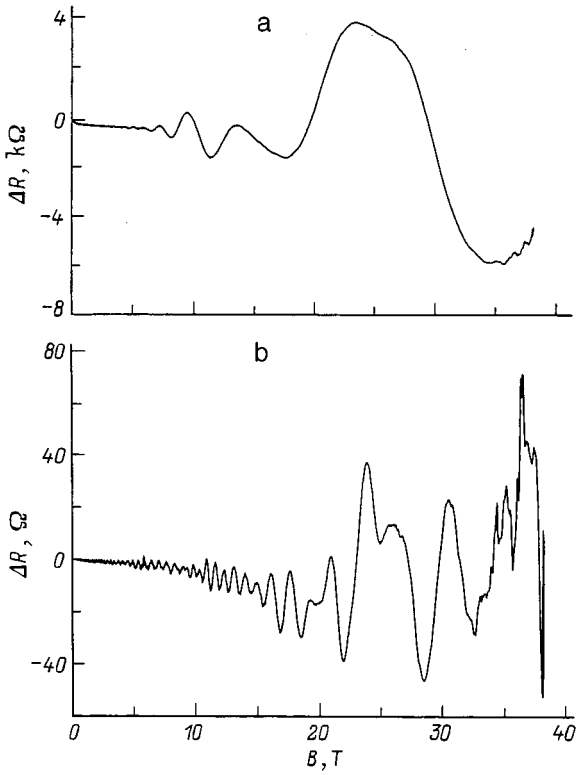

FIG. 2. Dependence of the change in resistance $\Delta R=R(B)-R(0)$ on the magnetic induction B at $T=4.2$ K for samples 2 (a) and 6 (b).

8×10^{12} cm^{-2}, which is comparable to the limiting electron concentration for silicon δ-doped GaAs structures.[4–6] However, when the concentration of tin introduced is increased further, the free-electron concentration increases significantly (sample 6). The saturation of the concentration of free carriers in GaAs (δ-Si) structures is usually attributed to the filling of *DX* centers[5,7] or an increase in the number of compensating defects[8,9] as the dopant concentration rises. It can be assumed that the energy of the *DX* level relative to the Γ conduction band edge increases at doping levels as high as in sample 6 (Refs. 10 and 11) and that different defects roughly compensate for the donor tin atoms.

When the electron mobilities in the quantum-well subbands are determined, it is important to distinguish the transport relaxation times from the quantum relaxation times.[12–14] The transport momentum relaxation time τ_t of an electron is determined by the mean time between events of elastic scattering on impurities that significantly alter the direction of the momentum and can be written in the form

$$\frac{1}{\tau_t}=\int_0^{\pi}\sigma(\varphi)(1-\cos\varphi)\,d\varphi, \tag{1}$$

where $\sigma(\varphi)$ is proportional to the probability of scattering into the angle φ per unit time in the plane of the δ layer. The quantum lifetime (one-particle relaxation time) is obtained by averaging the time between any scattering events and is given by the expression

$$\frac{1}{\tau_q}=\int_0^{\pi}\sigma(\varphi)\,d\varphi. \tag{2}$$

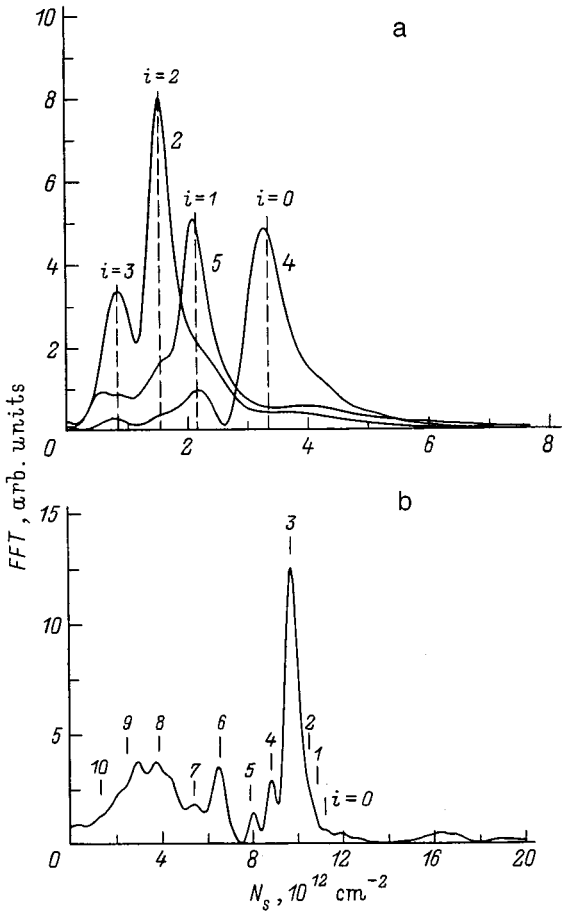

FIG. 3. Fourier spectra of the oscillations of the magnetoresistance in a reversed magnetic field for samples 2, 4, and 5 (a) and sample 6 (b). The arrows in part *b* show the concentrations corresponding to the calculated energies of the quantum-well subbands.

Because of the multiplier $(1-\cos\varphi)$ in the expression for τ_t, the transport scattering time can differ from the quantum analog. For isotropic scattering, for example, on phonons, these scattering times are equal. However, in the case of Coulomb scattering on ionized impurities, the cross section $\sigma(\varphi)$ is large for scattering into small angles; therefore, τ_t can be several times greater than τ_q.

An analysis of the magnetic-field dependence of the amplitude of the Shubnikov–de Haas oscillations makes it possible to determine the quantum mobilities $\mu_q = e/m^* \tau_q$ of electrons in each of the quantum-well subbands.[13] For this purpose, the corresponding frequencies are isolated in the Shubnikov–de Haas oscillations by a digital filter,[15] and a Dingle plot is constructed.[16] The quantum mobilities obtained increase in all the samples from approximately 600 $\text{cm}^2/(\text{V}\cdot\text{s})$ in the lower quantum-well subbands to 2100 $\text{cm}^2/(\text{V}\cdot\text{s})$ in the upper subbands (see Table II). These values are consistent with the mobility values obtained for silicon δ-doped GaAs structures.[17,18]

4. ENERGY SPECTRUM AND PHOTOLUMINESCENCE OF GaAs(δ-Sn) STRUCTURES

The band diagrams, wave functions, and electron concentrations in the quantum-well subbands were calculated by finding a self-consistent solution of the Schrödinger and Poisson equations by analogy with the calculations performed in Ref. 17. The nonparabolicity of the Γ conduction band was taken into account by substituting the mean square of the wave vector $\langle k_z^2\rangle_i = \int_{-\infty}^{\infty}\psi_i(-d^2/dz^2)\psi_i\,dz$ into the dispersion relation according to Ref. 19, permitting a calculation of the density of states in the ith subband. The thickness of the δ layer of ionized tin atoms, which served as a

TABLE II. Electron concentrations n_{SdH} and quantum mobilities μ_q^{SdH} in different subbands determined from the Shubnikov–de Haas effect at 4.2 K, concentrations N_S obtained from self-consistent calculations, quantum mobilities μ_q^t of electrons calculated for scattering on ionized impurities with allowance for intersubband scattering, and experimental ($B_\parallel$) and calculated ($B_\parallel^t$) values of the parallel magnetic induction at which emptying of the subbands occurs.

Sample No.	Subband number i	n_{SdH}, 10^{12}cm^{-2}	N_S, 10^{12}cm^{-2}	μ_q^{SdH}, $\text{cm}^2/(\text{V}\cdot\text{s})$	μ_q^t, $\text{cm}^2/(\text{V}\cdot\text{s})$	$B_\parallel$, T	$B_\parallel^t$, T
	0	1.76	1.75	1340	790	⋯	⋯
1	1	0.99	0.99	1450	900	18.6	20.5
	2	⋯	0.28	⋯	1120	4	7.4
	0	3.91	3.97	570	570	⋯	⋯
5	1	2.12	2.42	1100	740	33.4	41.7
	2	1.49	1.12	1630	1470	18.4	18.1
	3	0.57	0.33	2060	1830	5.6	6.3
	0	⋯	11.06	⋯	217	⋯	⋯
	1	⋯	10.80	⋯	217	⋯	⋯
	2	⋯	10.38	⋯	218	⋯	⋯
	3	9.75	9.75	1370	220	⋯	⋯
	4	8.84	8.87	1590	225	⋯	43.9
6	5	8.04	7.84	1910	236	36.3	34.1
	6	6.54	6.68	1330	258	29.6	28.7
	7	5.39	5.36	–	295	24.7	23.3
	8	3.76	3.91	–	359	19.7	17.8
	9	2.95	2.49	–	461	13.0	12.5
	10	–	1.32	–	509	7.6	8.0

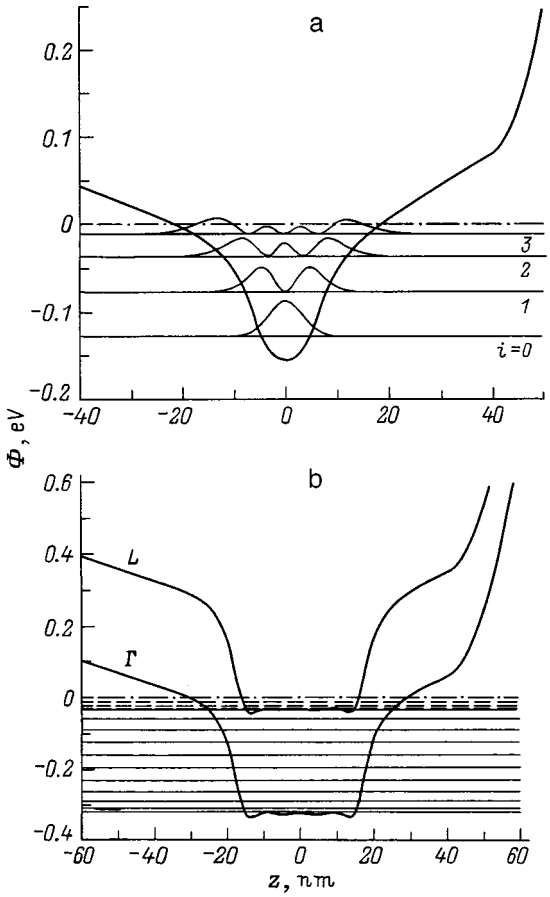

FIG. 4. Band diagrams for samples 5 (a) and 6 (b). The energy is measured relative to the Fermi level (dot-dashed line). The free surface of the samples is located at $z=60$ nm. The squares of the electronic wave functions in the subbands are also shown for sample 5. The energy levels at the L point in sample 6 are indicated by dashed lines.

fitting parameter in the calculations,[20] was found to be approximately equal to 16 nm for samples 1–5. Although such a δ layer thickness is higher than the values for silicon δ-doped structures,[4,7,21] it is small for tin.[1] The calculated two-dimensional electron concentrations in the quantum-well subbands are listed in Table II. Figure 4a shows the band diagram calculated for sample 5. It was taken into account in the calculations that the Fermi level is pinned on the free surface of the sample at a level 0.74 eV below the bottom of the conduction band[22] and in the semi-insulating substrate at the level for chromium (0.75 eV below the conduction band[23]).

In sample 6, which has the highest tin concentration $N_D=2.67\times10^{14}\,\mathrm{cm}^{-2}$ and a Hall concentration $n_H=8.35\times10^{13}\,\mathrm{cm}^{-2}$, the L conduction band should also be filled with electrons at low temperatures (according to Ref. 5, in the case of an ideally narrow δ layer this occurs when the concentration of the ionized impurity is above $N_D=1.6\times10^{13}\,\mathrm{cm}^{-2}$ and the electron concentration in the lowest subband is greater than $9.3\times10^{12}\,\mathrm{cm}^{-2}$). In the case of several filled subbands, the Hall concentration is averaged over all the subbands:

$$n_H=\frac{\left(\sum_i n_i\mu_{ti}\right)^2}{\sum_i n_i\mu_{ti}^2}, \tag{3}$$

where n_i is the electron concentration, and μ_{ti} is the transport mobility in the ith subband. As a result, the value of n_H is less than the total electron concentration in all the subbands determined from the Shubnikov–de Haas effect; therefore, in order to achieve such a high value of n_H, sample 6 must have at least three subbands with a concentration greater than $10^{13}\,\mathrm{cm}^{-2}$, which are weakly manifested in the range of magnetic fields investigated (see Fig. 3b). The electrons at the L point should not make a significant contribution to the value of n_H due to their low mobility. The following parameters of the electron effective masses at the L point for the (001) plane (Ref. 5) were used in the self-consistent calculation: for motion in the quantization direction $m_z=0.11m_0$, and for motion in the plane of the layer (the xy plane) $m_x=0.075m_0$ and $m_y=1.29m_0$. In this case the density-of-states effective mass $m_{ds}=(m_xm_y)^{1/2}=0.38m_0$, and there are four equivalent ellipsoids of constant energy (the degree of degeneracy $g_v=4$). The energies of the size-quantized subbands at the L point were calculated at a potential displaced along the energy scale by $E_{L-\Gamma}=290$ meV above the Γ point. The X point was neglected in the calculations, since $E_{X-\Gamma}=460$ meV. The potential curve at the Γ and L points was obtained by solving the Poisson equation for the total charge distribution, which consists of both the filled electronic states at the Γ and L points and the stationary positive charge of the ionized tin donors. The calculated band diagram for sample 6 is presented in Fig. 4b. The electron concentrations at the Γ point obtained for a thickness of a δ layer of ionized impurities equal to 34 nm are roughly equal to the observed concentrations in the Fourier spectrum (Fig. 3b and Table II). The concentrations in the three lowest subbands are very close to one another, and, therefore, the corresponding peaks merge to form a single broad peak near $1.1\times10^{13}\,\mathrm{cm}^{-2}$ in Fig. 3b; these peaks therefore cannot be clearly distinguished separately in the Fourier spectrum. The calculated electron concentrations in the three subbands at the L point are equal to 2.0×10^{13}, 1.54×10^{13}, and $7.8\times10^{12}\,\mathrm{cm}^{-2}$. The total free-electron concentration in this sample is at least 4 times greater than the maximum achievable concentration for silicon δ-doped GaAs structures[6] when the thickness of the δ layer is small for tin.[1]

Low-temperature photoluminescence provides an important experimental technique for investigating two-dimensional electron systems. However, investigating the photoluminescence of δ-doped structures is complicated by the fact that the potential retaining electrons in the quantum-well subbands is repulsive toward holes. This repulsion can reduce the overlap between the electron and hole wave functions and can consequently lower the photoluminescence intensity.[24,25]

Figure 5 presents the photoluminescence emission spectra of samples 3, 5, and 6, as well as a control sample with-

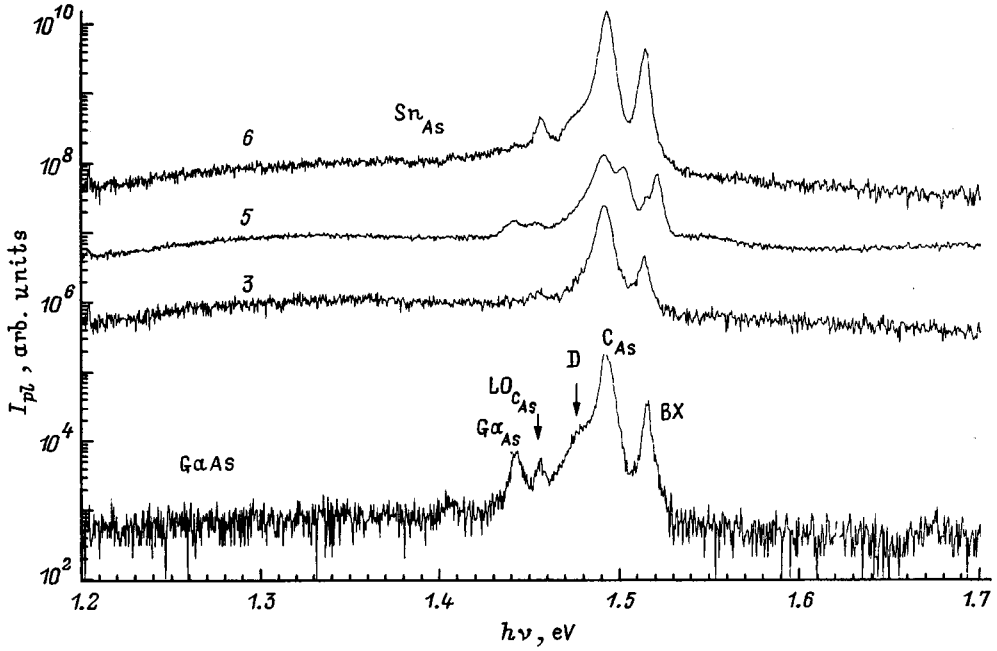

FIG. 5. Photoluminescence spectra of samples 3, 5, and 6 and of the control sample of GaAs without a δ layer at $T=4.2$ K. The positions of the maxima are explained in the text.

out a δ layer. The control sample was obtained by etching away the upper layers of sample 1, which contains a δ layer, to a depth of 100 nm. The low-temperature photoluminescence spectra of the GaAs sample without a δ layer contains characteristic lines with an energy of 1.514 eV, which corresponds to the recombination of excitons bound to a neutral donor; a line with an energy of 1.492 eV, which corresponds to a radiative electronic transition to a carbon acceptor level, and its LO-phonon replica with an energy of 1.456 eV; and a line with an energy of 1.442 eV (a Ga defect in the As sublattice).[26,27] The spectral feature at 1.478 eV is caused by recombination of a bound exciton involving an LO phonon, as well as recombination at defects appearing during growth by molecular-beam epitaxy.

For structures with δ layers of different concentrations the form of the photoluminescence spectrum varies as the doping level of the δ layer increases. A broad band with a maximum at 1.35 eV (see Fig. 5), which is caused by a radiative transition to a Sn acceptor level localized in the region of the δ layer, appears. The intensity of this band increases with increasing tin concentration. In addition, the ratio between the intensities of the lines characteristic of the sample without a δ layer described above varies, and new spectral features, which can be attributed to the recombination of electrons from quantum-well levels in the δ layer and photogenerated holes localized near the sample surface, appear.[24] The features caused by the quantum-well levels are especially pronounced for sample 5 (Fig. 6, the peaks with energies equal to 1.521 and 1.502 eV). These features can most probably be assigned to electronic transitions from the upper quantum-well levels, since the wave functions of the upper subbands extend far from the midplane of the δ layer and their overlap with the hole wave functions is greater than that for the lower subbands. The energy difference between the upper $i=2$ and $i=3$ subbands obtained for this sample in a self-consistent calculation is equal to 25 meV, which roughly coincides with the difference between the new photoluminescence lines. We also note that, along with the recombination channel just described, the recombination of electrons from the upper $i=3$ electronic level and holes localized at a carbon acceptor can make a contribution to the line at 1.502 eV.

The wave functions found in the self-consistent calculations were used to calculate the low-temperature quantum mobilities of electrons for multisubband scattering at ionized impurities,[28–30] which are listed in Table II. The screening of the scattering Coulomb potential was taken into account in the random-phase approximation.[28] It can be seen from the

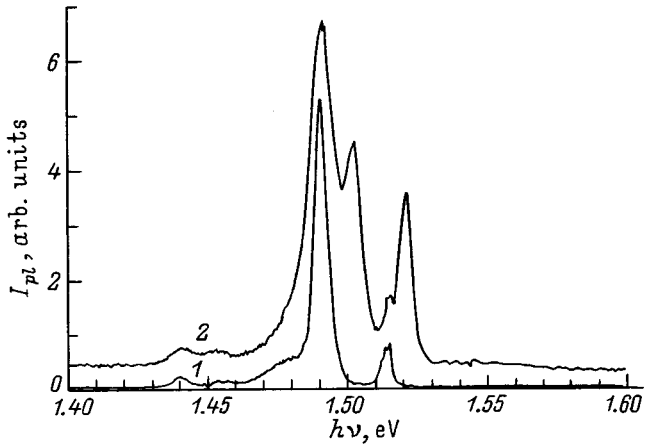

FIG. 6. Isolated parts of the photoluminescence spectra of the control sample without a δ layer (*1*) and sample 5 (*2*) at $T=4.2$ K. The photoluminescence intensities are the same as in Fig. 5.

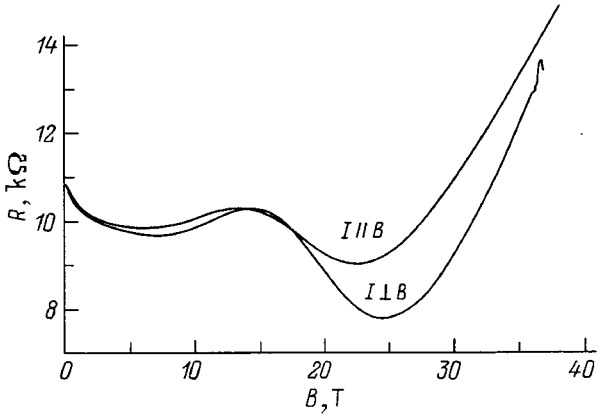

FIG. 7. Resistance of sample 1 in a magnetic field parallel to the δ layer for two orientations of the current through the sample relative to the magnetic field.

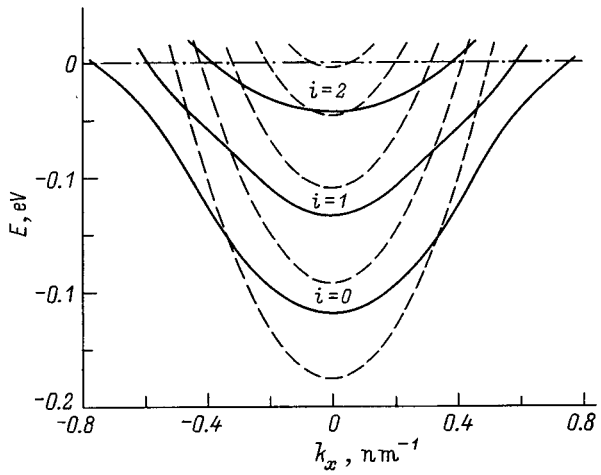

FIG. 8. Quantum-well energy subbands in sample 2 in the absence of a magnetic field (dashed lines) and in a field with $B=18$ T (solid lines).

numerical calculations (see Table II) that the electron mobilities increase with the subband number i, since the mean distance from electrons to impurities is greater in the upper subbands. The calculated quantum mobilities in samples 1–5 were somewhat smaller than the values determined from the Shubnikov–de Haas effect (see Table II) due to the partial correlation in the distribution of the ionized impurities.[31,32] In sample 6 the quantum mobilities of electrons determined from the Shubnikov–de Haas effect are more than six times greater than the calculated quantum mobilities. This is attributable to the strong screening of the ionized impurities by the L-band electrons, which have a large effective mass (this screening was disregarded in the calculations), as well as by stronger correlation of the impurities than in samples 1–5.

5. RESISTANCE OSCILLATIONS IN A MAGNETIC FIELD PARALLEL TO THE δ LAYER

Measuring the Shubnikov–de Haas effect is the principal method for determining the electron concentrations in quantum-well subbands of two-dimensional systems. However, in δ-doped structures the upper subbands have low concentrations of electrons, from which oscillations are difficult to see when the Shubnikov–de Haas effect is measured. The diamagnetic Shubnikov–de Haas effect, under which the magnetic field is directed in the plane of the δ layer, however, permits exact determination of the number of filled subbands[33] and is a useful tool for investigating multisubband two-dimensional systems. As an example, Fig. 7 presents the resistance oscillations of sample 1 in a magnetic field parallel to the surface for currents parallel and perpendicular to the magnetic field.

If the magnetic induction B is directed along the y axis and the vector potential is $\mathbf{A}=(Bz,0,0)$, the Schrödinger equation has the form[34]

$$\left[\frac{p_y^2}{2m^*}+\frac{1}{2m^*}(p_x+ezB)^2-\frac{\hbar^2}{2m^*}\frac{\partial^2}{\partial z^2}+\Phi(z)\right]\Psi=E\Psi. \tag{4}$$

Here the potential $\Phi(z)$ is the sum of the electrostatic potential U_H determined from the Poisson equation

$$\frac{d^2U_H(z)}{dz^2}=-\frac{e^2}{\varepsilon_0\varepsilon}\left[\sum n_i\psi_i^2(z)-N(z)\right], \tag{5}$$

where $\varepsilon=13.18$ is the dielectric constant of GaAs, $N(z)$ is the volume concentration of ionized donors, and $n_i=m^*/\pi\hbar^2(E_F-E_i)$ is the two-dimensional electron concentration in the ith subband, and of the exchange-correlation potential $U_{\rm xc}$ (Ref. 35)

$$U_{\rm xc}=-\left[1+0.0545r_S\ln\left(1+\frac{11.4}{r_S}\right)\right]\frac{2}{\pi\alpha r_S}Ry^*, \tag{6}$$

where

$$\alpha=\left(\frac{4}{9\pi}\right)^{1/3},\quad r_S=\left(\frac{4\pi a_B^3 n(z)}{3}\right)^{-1/3},$$

$$a_B^*=\frac{4\pi\varepsilon_0\varepsilon\hbar^2}{m^*e^2},\quad Ry^*=\frac{e^2}{8\pi\varepsilon_0\varepsilon a_B^*},$$

$n(z)$ is volume concentration of electrons. The self-consistent solution can be written in the form

$$E=E_i(k_x)+\frac{\hbar^2}{2m^*}k_y^2. \tag{7}$$

The calculations were performed for the parabolic case, and the electron effective mass in all the subbands was assumed to be $m^*=0.07m_0$. Figure 8 presents plots of $E_i(k_x)$ for $B=0$ and $B=18$ T in the case of sample 2. It is seen that in such a magnetic field the $i=4$ and $i=3$ subbands are pushed upward above the Fermi level and emptied; here the electrons are redistributed among the remaining three subbands in the varying self-consistent potential $\Phi(z)$. As the magnetic field is increased, the subbands are shifted toward the Fermi level, and the total density of states $g(B)$ increases, but it subsequently drops sharply when the energy of each successive subband passes through the Fermi level. The increase in the density of states and emptying of the subbands lead to oscillations of the magnetoresistance (Fig. 9). The calculated values of the magnetic induction $B_\parallel^f$ at which emp-

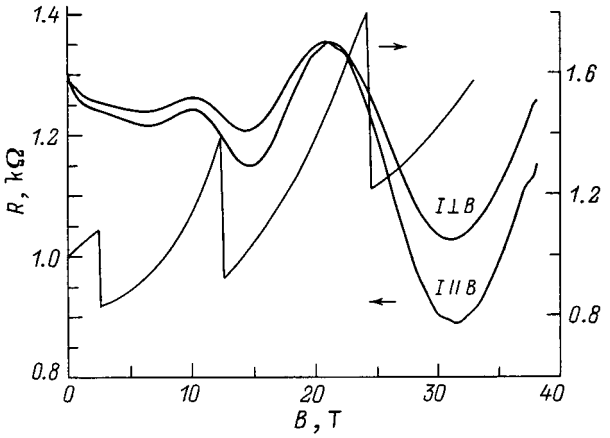

FIG. 9. Dependence of the resistance of sample 2 on the magnetic induction parallel to the δ layer for two orientations of the current through the sample relative to the magnetic field and ratio of the calculated density of states at the Fermi level $g(B)$ to the density of states in the absence of a magnetic field $g(0)$.

tying of the respective quantum-well subbands occurs and the experimental values of $B_\parallel$ determined from the minima of the first derivative of the magnetoresistance[34] closely coincide (see Table II). The small difference between the calculated and experimentally determined values of $B_\parallel$ can be attributed to the fact that the crossing of the Fermi level by the subbands is accompanied by changes not only in the density of states, but also in the electron mobilities due to intersubband scattering.[36] The positions of the resistance maxima depend weakly on the direction of the current flowing through the sample relative to the parallel magnetic field (Figs. 7 and 9), as in the case of thick silicon δ layers.[34]

In sample 6 the energy position of the subbands is determined to a considerable degree by the nonparabolicity of the Γ conduction band: according to the calculations, the electron effective mass increases from $0.083m_0$ in the lowest subband to $0.1m_0$ in the highest. Perturbation theory can be used to estimate the values of the parallel magnetic induction $B_\parallel$ at which emptying of the subbands occurs in this sample. Emptying of a subband occurs when the diamagnetic energy shift $e^2B_\parallel^2/2m^*\langle z_i^2\rangle$ equals the energy of the bottom of the respective subband $E_i=\pi\hbar^2/m^*n_i$. We thus obtain

$$B_\parallel=\sqrt{\frac{2\pi\hbar^2 n_i}{e^2\langle z_i^2\rangle}}. \tag{8}$$

Formula (8) does not contain the effective mass and agrees fairly well with the results of the exact calculation.[37] The values of the magnetic induction $B_\parallel$ thus obtained for sample 6 agree well with the experimentally determined values (see Table II), attesting to the correctness of the description of the upper subbands in this sample.

6. CONCLUSIONS

The transport and optical properties of GaAs(δ-Sn) structures have been investigated as a function of the tin concentration. The calculated quantum mobilities of electrons in the quantum-well subbands agree fairly well with the corresponding values determined from the Shubnikov–de Haas effect. The maximum two-dimensional free-electron concentration obtained exceeds the limiting values for silicon δ-doped GaAs structures when the thickness of the tin δ layer is relatively small. At such high concentrations the L conduction band is filled with electrons. The calculated values of the parallel magnetic induction at which emptying of the subbands occurs closely coincide with the experimentally determined values.

We thank Dr. P. M. Koenraad for a useful discussion of the results of this work.

This work was carried out with support from the Russian Fund for Fundamental Research (Grants Nos. 97-02-17396, 96-02-18593a, and 98-02-17452) and the Dutch Organizations N.W.O and F.O.M.

[1] J. J. Harris, D. E. Ashenford, C. T. Foxon, P. J. Dobson, and B. A. Joyce, Appl. Phys. A: Solids Surf. **33**, 87 (1984).
[2] A. de Visser, V. I. Kadushkin, V. A. Kul'bachinskiĭ, V. G. Kytin, A. P. Senichkin, and E. L. Shangina, JETP Lett. **59**, 363 (1994).
[3] V. A. Kulbachinskii, R. A. Lunin, E. V. Bogdanov, V. G. Kytin, and A. P. Senichkin, Physica B **229**, 262 (1997).
[4] A. Zrenner, F. Koch, and K. Ploog, Surf. Sci. **196**, 671 (1988).
[5] A. Zrenner, F. Koch, R. L. Williams, R. A. Stradling, K. Ploog, and G. Weimann, Semicond. Sci. Technol. **3**, 1203 (1988).
[6] J. V. Thordson, T. G. Andersson, G. Swenson, and U. Rodervall, J. Cryst. Growth **175/176**, 234 (1997).
[7] S. P. Wilks, A. E. Cornish, M. Elliot *et al., J. Appl. Phys.* **76**, 3583 (1994).
[8] R. C. Newman, M. J. Ashwin, M. R. Fahy *et al., Phys. Rev. B* **54**, 8769 (1996).
[9] C. Domke, P. Ebert, M. Heinrich, and K. Urban, Phys. Rev. B **54**, 10 288 (1996).
[10] D. K. Maude, J. C. Portal, L. Dmowski *et al., Phys. Rev. Lett.* **59**, 815 (1987).
[11] P. M. Mooney, J. Appl. Phys. **67**, R1 (1990).
[12] P. M. Koenraad, in *Delta Doping of Semiconductors*, E. F. Schubert (Ed.), Cambridge University Press, Cambridge (1996), Chap. 17.
[13] P. M. Koenraad, A. F. W. van de Stadt, J. M. Shi *et al., Physica B* **211**, 462 (1995).
[14] P. T. Coleridge, R. Stoner, and R. Fletcher, Phys. Rev. B **39**, 1120 (1989).
[15] J. F. Kaiser and W. A. Reed, Rev. Sci. Instrum. **49**, 1103 (1978).
[16] P. T. Coleridge, Phys. Rev. B **44**, 3793 (1991).
[17] V. A. Kul'bachinskiĭ, R. A. Lunin, V. G. Kytin, A. S. Bugaev, and A. P. Senichkin, Zh. Éksp. Teor. Fiz. **110**, 1517 (1996) [JETP **83**, 841 (1996)].
[18] R. A. Lunin, V. G. Kytin, V. A. Kul'bachinskiĭ, and G. A. Mironova, Vestn. Mosk. Univ., Ser. 3: Fiz. Astron., No. **4**, 31 (1997).
[19] U. Rössler, Solid State Commun. **49**, 943 (1984).
[20] M. H. Degani, Phys. Rev. B **44**, 5580 (1991).
[21] E. F. Schubert, C. W. Tu, R. F. Kopf *et al., Appl. Phys. Lett.* **51**, 2592 (1989).
[22] T. M. Hsu, W.-H. Chang, D. H. Liao, and W. C. Lee, J. Appl. Phys. **84**, 1074 (1998).
[23] A. Chandra, C. E. C. Wood, D. W. Woodard, and L. F. Eastman, Solid-State Electron. **22**, 645 (1979).
[24] J. Wagner, A. Fischer, and K. Ploog, Phys. Rev. B **42**, 7280 (1990).
[25] J. Wagner and D. Richards, in *Delta Doping of Semiconductors*, E. F. Schubert (Ed.), Cambridge University Press, Cambridge (1996), Chap. 15.
[26] M. S. Skolnick, C. W. Tu, and T. D. Harris, Phys. Rev. B **33**, 8468 (1986).
[27] D. J. Ashen, P. J. Dean, D. T. J. Hurle *et al., J. Phys. Chem. Solids* **36**, 1041 (1975).
[28] G.-O. Hai, N. Studart, and F. M. Peeters, Phys. Rev. B **52**, 8363 (1995).
[29] L. R. Gonzalez, J. Krupski, and T. Szwacka, Phys. Rev. B **49**, 11 111 (1994).
[30] L. C. D. Goncalves and A. B. Henriques, Semicond. Sci. Technol. **12**, 203 (1997).
[31] J. M. Shi, P. M. Koenraad, A. F. W. van de Stadt *et al., Phys. Rev. B* **55**, 13 093 (1997).
[32] R. Shikler, M. Heiblum, and V. Umansky, Phys. Rev. B **55**, 15 427 (1997).

[33] H. Reisinger and F. Koch, Surf. Sci. **170**, 397 (1986).
[34] A. F. W. van de Stadt, R. Bogaerts, P. M. Koenraad *et al.*, Physica B **211**, 458 (1995).
[35] *Theory of the Inhomogeneous Electron Gas*, S. Lundqvist and N. H. March (Eds.) [Plenum Press, New York (1983); Mir, Moscow (1987)].
[36] J. M. Heisz and E. Zaremba, Phys. Rev. B **53**, 13 594 (1996).
[37] A. Zrenner, H. Reisinger, F. Koch, K. Ploog, and J. C. Maan, Phys. Rev. B **33**, 5607 (1986).

Translated by P. Shelnitz